

Molecular Dynamics during Crystallization of Poly(L-lactic acid) As Studied by Broad-Band Dielectric Relaxation Spectroscopy

Jovan Mijović* and Jo-Wing Sy

Department of Chemical Engineering and Chemistry and The Herman F. Mark Polymer Research Institute, Polytechnic University, Six MetroTech Center, Brooklyn, New York 11201

Received March 11, 2002; Revised Manuscript Received May 30, 2002

ABSTRACT: An investigation was carried out of the molecular dynamics of poly(L-lactic acid) *before, during, and after* crystallization. Experimental results were generated over a wide range of temperature and frequency by broad-band dielectric relaxation spectroscopy (DRS). An interesting finding is that the average relaxation time (defined as $\tau = 1/2\pi f_{\max}$, where f_{\max} is the frequency at maximum loss for the α process) does not vary with degree of crystallinity during melt and/or cold crystallization. Moreover, the temperature dependence of the average relaxation time for wholly amorphous and crystallized samples is well-described by a single Vogel–Fulcher–Tammann (VFT) functional form. The unchanged fragility suggests that the segmental dynamics are not sensitive to the different degree of crystallinity, implying that the relaxing segments are smaller than the thickness of the amorphous layers between lamellae. Apparently, the distance between lamellae is greater than the length of the primitive segment and the characteristic size of the cooperatively rearranging domain; the length scale of the α process is thence put at less than 4 nm.

Introduction

The effect that the crystalline phase exerts on the α dynamics in the amorphous phase during crystallization of polymers and low molecular weight materials is an interesting, fundamentally important, and incompletely understood problem. The work presented herein addresses this problem experimentally by utilizing broad-band dielectric relaxation spectroscopy (DRS) over a wide range of frequency and temperature to monitor dynamics during the melt and cold crystallization of poly(L-lactic acid) (PLA). To the best of our knowledge, this study marks the first time that high-frequency (up to 1.8 GHz) data of this kind have been generated and reported in the literature.

As a start, it is useful to ask how (and if) the segmental α process in a wholly amorphous but crystallizable polymer is altered once the crystals begin to form? This has been studied experimentally over a limited range of frequency and temperature by directly comparing the dielectric spectra of crystalline and wholly amorphous samples (in cases where a crystalline polymer could be rendered wholly amorphous) and/or by continuously monitoring the dielectric response during crystallization. The following general observations were made:^{1–5} (1) the *relaxation strength* of the α process decreases with increasing crystallinity and decreasing temperature, and (2) the *breadth* of the α process increases with increasing crystallinity. On the basis of those findings, two-phase and three-phase conceptual models have been put forward to explain the experimental results.² The former assume that the motions of polymer segments are frozen on the crystal surface whereas the latter allow for the existence of an amorphous interphase. Experimental evidence from dielectric measurements of crystalline polymers favors a two-phase model because only one relaxation associated with the amorphous phase has been seen, although

a broadening of the relaxation spectrum is often invoked as the reason for the inability to resolve two processes. In a seminal DRS study, Tidy and Williams⁶ reported that during isothermal crystallization of PET the “normal” amorphous phase disappears and a broader and slower “abnormal” relaxation appears in the amorphous phase. Relaxation slows down, and the distribution of relaxation times broadens as a result of the increasing variety of local environments seen by the molecules. Eventually, the initial α process disappears, and the new (slower) process becomes dominant. The origin of this new process was attributed to the relaxations within disordered regions that are restricted by the emerging ordered regions. Another scenario is based on the presence of a rigid amorphous phase.^{7,8} This concept was put forward to account for the portion of the amorphous phase that remains rigid above T_g and was later exploited by Huo and Cebe to describe their dielectric results for PEEK⁹ and PPS.¹⁰

Interestingly, however, the effect of crystallinity on the average relaxation time, τ (defined as $\tau = 1/2\pi f_{\max}$, where f_{\max} is the frequency at maximum loss), for the α process is found to be more complex, and the experimental results are seen to depend on the type of polymer investigated. In polymers with a high T_m and a rigid backbone, such as PET,⁶ PEEK,⁹ and PPS,¹⁰ the presence of crystals causes the relaxation time to increase. But in several flexible-chain homopolymers (PVDF¹¹ and PLA (this work)), homopolymer blends (PVDF/PMMA¹²) and blends containing block copolymers (PBT/PC¹³), the relaxation time was found to either remain unaffected or even decrease. How one can account for these different trends in τ is of interest.

The principal objectives of this study are (1) to investigate the effect of cold and melt crystallization on molecular (dipole) dynamics in PLA by DRS over a wide range of frequency (up to 12 decades) and temperature and (2) to elucidate the effect that the crystalline phase exerts on the α process *before, during, and after* crystallization by (a) comparing the dielectric response in

* To whom correspondence should be addressed. E-mail: jmijovic@poly.edu.

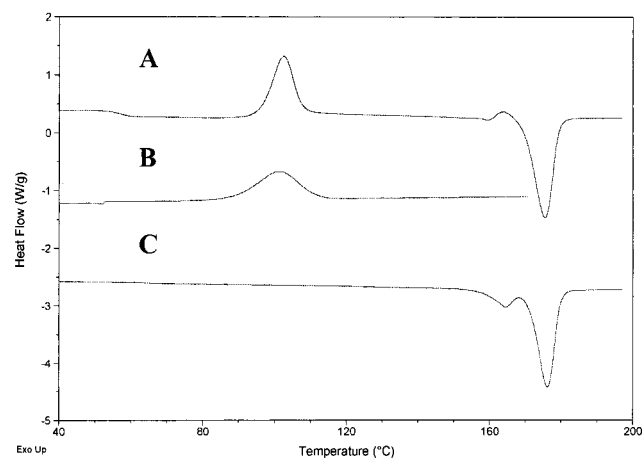


Figure 1. DSC thermograms of PLA (at 10 °C/min): A, heating following quenching into liquid nitrogen; B, cooling from the melt; C, heating following annealing at 150 °C for 2 h.

wholly amorphous and crystallized samples and (b) monitoring the dielectric response in-situ during melt and cold crystallization.

Experimental Section

The sample studied in this work, poly(L-lactic acid) (PLA), was synthesized at Polytechnic in the laboratory of Professor Richard Gross ($M_n = 34\,100$ g/mol; $PI = 1.9$). Our facility for DRS combines commercial and custom-made instruments that include (1) Novocontrol's α high-resolution dielectric analyzer (3 μ Hz–10 MHz), (2) Solartron 1260 impedance gain/phase analyzer (10 μ Hz–32 MHz), (3) Hewlett-Packard 4284A precision LCR meter (20 Hz–1 MHz), (4) Hewlett-Packard 8752A network analyzer (300 kHz–1.3 GHz), and (5) Hewlett-Packard 4291B RF impedance analyzer (1 MHz–1.8 GHz). All instruments are interfaced to computers and equipped with heating/cooling capabilities, including a custom-modified Novocontrol's Novocool system. Further details regarding the acquisition and evaluation of data are available elsewhere.¹⁴ Supporting evidence was obtained from DSC scans (TA instrument's DSC model 2920 at 10 °C/min) and optical microscopy (Nikon HFX-II optical microscope).

Results and Discussion

Two approaches are undertaken to investigate the effect of crystallization on the molecular dynamics of PLA by DRS. The first approach consists of comparing the relaxation spectra of wholly amorphous and crystallized samples. The second approach focuses on in-situ monitoring of the dielectric response during isothermal (cold and melt) crystallization. Before presenting the DRS results, we briefly review the thermal behavior of PLA as evaluated by DSC.

DSC thermograms for three different thermal histories are shown in Figure 1. Trace A was obtained on heating a sample quenched from the melt into liquid nitrogen (rendering the sample wholly amorphous). The glass transition is observed at 57 °C, while cold crystallization and melting occur at 102 and 175 °C, respectively. Trace B was obtained on cooling from the melt. The crystallization temperature is detected at 99 °C, similar to that for cold crystallization. Crystallized samples were prepared by cooling the melt at 10 °C/min to 150 °C and annealing for 2 h at that temperature. A DSC scan of the annealed sample is shown in trace C. Neither glass transition nor crystallization exotherms were observed (within the resolution of the instrument), and hence the annealed sample was considered (fully)

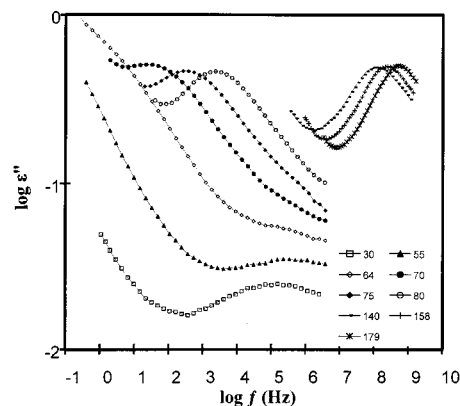


Figure 2. Dielectric loss in the frequency domain with temperature as a parameter for *wholly amorphous* PLA.

crystallized at temperature below 150 °C. We are aware of the arguments concerning continuing crystallization and metastability of crystalline polymers,¹⁵ but there were no changes in crystallinity in our sample with time well beyond the time span of the experiment and it is in that context that the label “crystallized” is used here.

We now present the dielectric results.¹⁶ The relaxation spectra for the *wholly amorphous* sample are examined first. Since the permittivity and loss are related by the Kramers–Kronig transform, only the loss data are presented in the figures. Dielectric loss in the frequency domain with temperature as a parameter for wholly amorphous PLA is shown in Figure 2. The data below 80 °C were obtained from the frequency sweeps of a quenched sample prior to the onset of crystallization. Data at high temperature were collected from the melt, cooled to below the nominal T_m but before the onset of crystallization. Solid lines are the guides for the eye. The gap in the data in Figure 2 (between approximately 80 and 140 °C) represents the region where crystallization cannot be neglected on the time scale of dielectric experiments, and hence the sample cannot be rendered wholly amorphous. The α process is clearly seen between 70 and 80 °C. Below 70 °C, however, the α process overlaps with conductivity, and a physically meaningful deconvolution is not feasible. A low-intensity β relaxation is observed below T_g (see data at 30 and 55 °C). It should be pointed out that a relaxation related to the normal mode (type A dipoles are present in polylactones^{17,18}) was not detected in this sample. That may be due to two factors: (1) a high conductivity at low frequency that masks the normal mode and (2) a relatively high molecular weight that increases considerably the relaxation time of the normal mode. The α process is thermodielectrically complex, and the loss peak becomes slightly narrower with increasing temperature. Fits of data to the KWW functional form were also made, and the KWW β exponent was found to increase from 0.46 at 80 °C to 0.53 at 150 °C.

Dielectric loss in the frequency domain for a *crystallized* sample is shown in Figure 3. The intensity of the loss peak (associated with segmental motions in the amorphous phase) and the dielectric relaxation strength decrease with decreasing temperature. The α process is thermodielectrically complex; the loss peak broadens with decreasing temperature, and it is difficult to measure below 90 °C due to its breadth and the dc conductivity. Also, the relaxations associated with the glass transition become highly suppressed on approach-

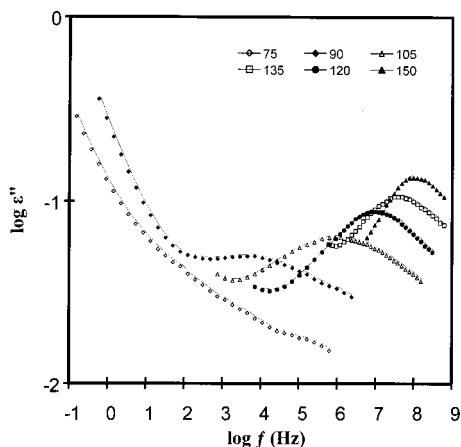


Figure 3. Dielectric loss in the frequency domain with temperature as a parameter for *fully crystalline* PLA.

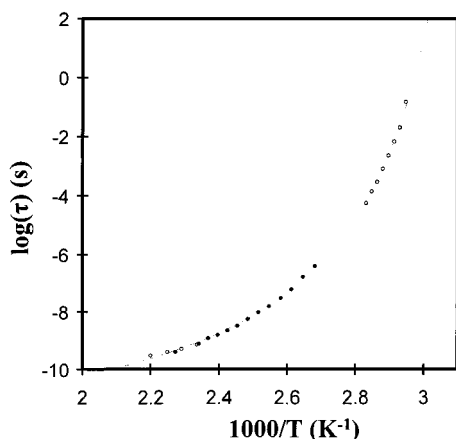


Figure 4. Average relaxation time as a function of reciprocal temperature for wholly amorphous (open circle) and crystalline (solid circle) PLA.

ing the T_g . This observation is in agreement with the DSC data for the annealed sample (trace C, Figure 1) that show no evidence of a T_g endotherm.

The temperature dependence of the relaxation time for *wholly amorphous and crystallized* samples is examined next. In Figure 4 we plot the average relaxation time (determined as $\tau = 1/2\pi f_{\max}$) as a function of reciprocal temperature for wholly amorphous (open circles) and crystallized (filled circles) samples. It is very interesting to note that all data points fall on the same curve, indicating that the temperature dependence of the average relaxation time is not affected by the presence of crystals. It is well-known that the α process in glass-formers deviates from a thermally activated Arrhenius functional form and that much stronger temperature dependence is observed. Such behavior is generally modeled by the Vogel–Fulcher–Tammann (VFT) equation, represented by the solid line in Figure 4. An excellent fit was obtained. The VFT fit parameters are τ_0 (attempt frequency) = 10^{-14} s, $B = 1516$ K, and T_0 (Vogel temperature) = 286.5 K. It is clear that the relaxation time follows the VFT relation regardless of the presence and/or absence of the crystalline phase. This is actually unusual because the VFT functional form is widely believed to hold only for amorphous systems.

Since the molecular origin of a relaxation process is generally related to its morphological milieu, it was anticipated that much could be learned about relaxation

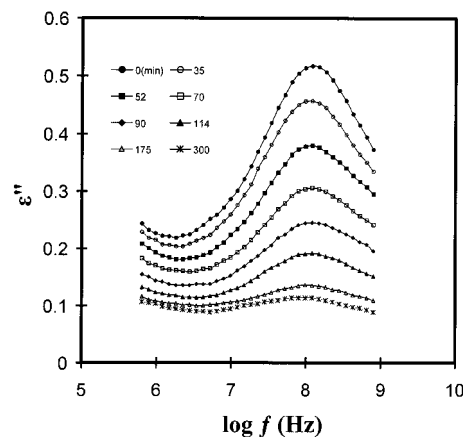


Figure 5. Dielectric loss in the frequency domain at different times during melt crystallization of PLA at 140 °C.

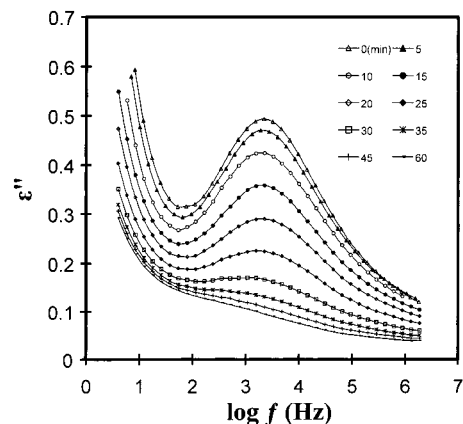


Figure 6. Dielectric loss in the frequency domain at different times during cold crystallization of PLA at 80 °C.

dynamics by monitoring the dielectric response *during* the temporal evolution of crystalline morphology. This goal was accomplished by conducting in-situ real-time DRS measurements during melt and cold crystallization of PLA. The results obtained from melt crystallization are presented first. Figure 5 shows dielectric loss in the frequency domain at different times during crystallization at 140 °C ($T_c = 140$ °C). To the best of our knowledge, this marks the first time that high-frequency measurements (1 MHz to 1.8 GHz) of the α dynamics during crystallization were reported. We emphasize that the spectra recorded in each sweep are representative of an *isostructure* (constant degree of crystallinity) at a given stage of crystallization, because the time scale for a sweep is short (less than 40 s) in comparison with the time scale for crystallization at T_c . As shown in Figure 5, the intensity and the relaxation strength of the α process drop dramatically during crystallization (ϵ'' decreases from 0.52 prior to the onset of crystallization to 0.12 at the end of crystallization). Remarkably, however, the location of the peak (at ca. 0.1 GHz) remains virtually unchanged throughout crystallization, indicating that the average relaxation time ($\tau = 1.6$ ns) is independent of the degree of crystallinity. A small shift toward low frequency is noted after 300 h at T_c , but a physically meaningful quantification (spectral deconvolution) is difficult at such advanced stage of crystallization. Similar results were obtained for cold crystallization at 80 °C, as shown in Figure 6, where we again see that the magnitude of the loss peak and the relaxation strength decrease while

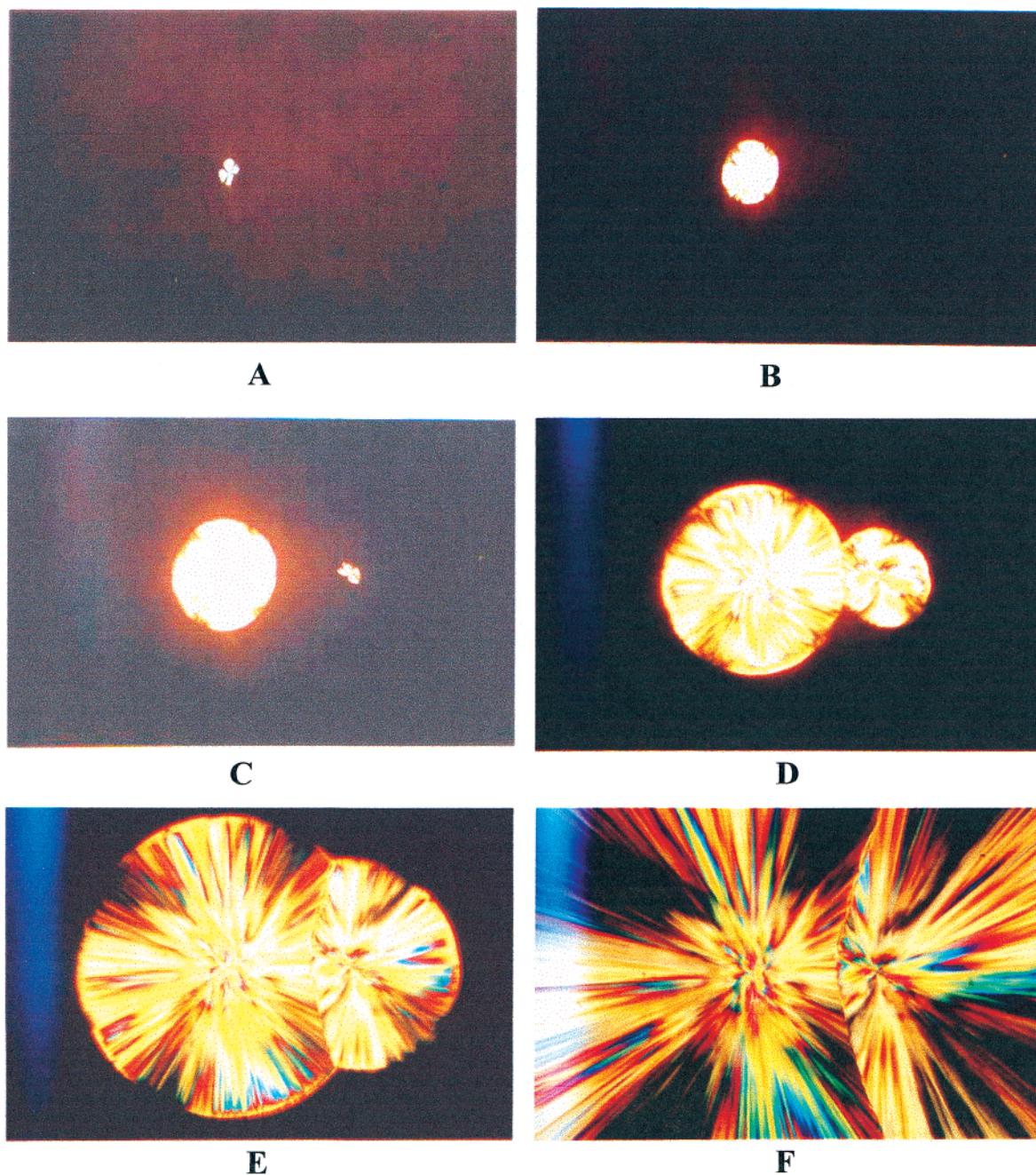


Figure 7. Polarized optical micrographs obtained during melt crystallization of PLA at 140 °C: A, 5 min; B, 10 min; C, 14 min; D, 21 min; E, 30 min; F, 60 min.

the frequency at maximum loss remains unchanged as crystallization progresses. Spectra of both melt and cold crystallized samples broaden during crystallization. The low-frequency shoulder at the end of cold crystallization may reflect the Maxwell–Wagner–Sillars or interfacial polarization. Note that the values of τ obtained from Figure 5 (τ at 140 °C) and Figure 6 (τ at 80 °C) fall on the VFT fit of Figure 4, and hence the dynamics data extracted from cold and melt crystallization are in excellent agreement with the data obtained on wholly amorphous and crystallized samples. We saw no need to resort to two VFT functions (the Stickel plot) although such a trend could not be ruled out a priori. To facilitate the visualization of the development of crystals, we show in Figures 7 and 8 a series of optical micrographs taken at different times during melt and cold crystallization at the conditions of Figures 5 and 6 (i.e., at 140 and 80

°C, respectively). Note that the resulting morphologies are quite different and that larger and more perfect spherulites are formed during melt crystallization. A grainlike morphology is observed during cold crystallization, probably due to a higher nucleation rate. No further exploration of the morphological details vis-à-vis the dynamics was made in this study. We also stress that we were not principally concerned here with the kinetics of crystallization, though it is obvious that the data of Figures 5 and 6 are conducive to this type of analysis. One such example can be found in the excellent recent study of molecular dynamics and crystallization kinetics of chiral isooctyloxycyanobiphenyl by DRS.¹⁹

Although the principal goal of this study was of experimental nature, a comment regarding the underlying physics is in order. The molecular dynamics in

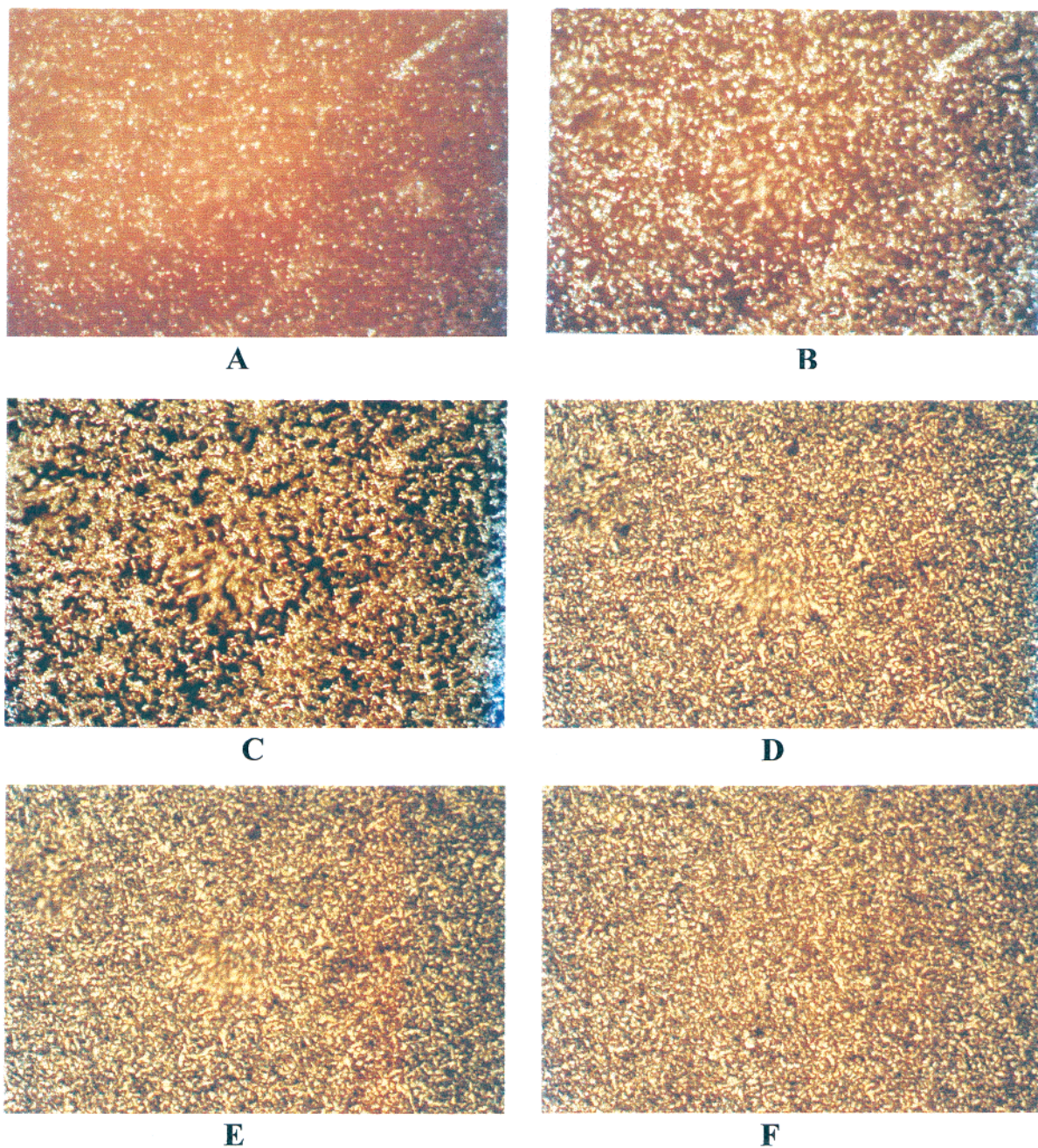


Figure 8. Polarized optical micrographs obtained during cold crystallization of PLA at 80 °C: A, 3 min; B, 6 min; C, 9 min; D, 15 min; E, 25 min; F, 45 min.

crystalline polymer are complex, and the experimentally observed differences in various polymers are a consequence of their different molecular architecture. Broadly speaking, the hindrance to α the dynamics imposed by the crystalline phase cannot be neglected; it is reflected in the reduction of the dielectric relaxation strength by an amount larger than the mere depletion of the amorphous portion during crystallization estimated from the DSC data. But if the restricted mobility by crystals were the only important factor, one would arrive at a straightforward conclusion that the dynamics in the amorphous phase must slow and that the average relaxation time must increase as more crystals form. That, however, is not always the case, as demonstrated in this study by (1) the unchanged location of the maximum at loss peak during melt and cold crystallization and (2) the fact that the same VFT function can describe wholly amorphous and crystallized samples.

There is another important factor that ought to be considered in explaining our (and others') findings, namely the effect of confinement that crystalline lamellae exert on the dynamics of the amorphous phase. The effect of confinement on the α dynamics was addressed in recent years in a number of studies of the dynamics of (mostly) low molecular liquids in confined nanoporous spaces of the order of 2.5–10 nm.^{20–23} And although some lingering controversy persists as regards the direction of the shift in T_g of the confined liquid, several investigators report evidence of a two-tier dynamics associated with a layer near the surface and a bulklike response away from the surface. The origin of the "interfacial" relaxation, that exhibits slower dynamics, is in the interactions of liquid molecules with the pore surface. But what if these surface interactions are eliminated? That was realized by Kremer and co-workers,²² who coated the pore surface with a hydro-

phobic fluid and studied the α dynamics of salol contained in pores ranging in size from 2.5 to 7.5 nm. They reported that (1) the interfacial relaxation was completely suppressed in coated pores, (2) with decreasing temperature the relaxation rate in confined space shifts to higher frequency compared to the bulk liquid, and (3) the shift in the relaxation rate is more pronounced in small pores. Kremer et al. offered an explanation of their findings based on the classic Adam–Gibbs²⁴ concept of cooperativity of the α dynamics in glass formers characterized by dynamic distribution of domain sizes. In a dynamically heterogeneous environment the suppression of relaxations by the emerging confinement increases with increasing domain size; the larger the domain, the stronger the effect on relaxation. Consequently, segmental motions with longer relaxation times will be preferentially suppressed, and the relaxation spectrum of a confined system will differ from that in the bulk. It is important to emphasize, however, that the confinement effect does not necessarily speed up the relaxation process (as a decrease in τ would suggest) but that the suppression of large-scale motions (longer τ) shifts the relaxation spectrum toward higher frequency. Since the decrease in the mobility and the suppression of slower relaxations have opposite effects on the relaxation spectrum, it is the interplay between these two phenomena that will determine whether the average relaxation time will increase or decrease. It should be also pointed out that the temperature dependence of these two phenomena is different. We believe that temperature affects suppression of relaxations by confinement more than molecular mobility. This should be studied further by measurements over a wide range of temperature that should include the crossover from the melt to the crystalline state and from the α process to the β process.

The experimentally observed constancy of the average relaxation time during crystallization (Figures 5 and 6) was intriguing, and an explanation was sought. Considering the effect of confinement, one possible scenario would call for the decrease in the mobility and the suppression of slower relaxations to balance each other, though that is intuitively unappealing. A more likely cause for the constancy of the average relaxation time is that the critical size of the cooperatively rearranging domain remains smaller than the distance between crystalline lamellae, and hence the confinement effect never sets in. Of course, that begs the question of the characteristic length scale for cooperativity and how it changes with the depletion of the amorphous phase during crystallization? Schick and Donth asked that question in their excellent study of the α dynamics in crystalline poly(ethylene terephthalate).²⁵ PET was crystallized under different conditions in order to induce morphology with a different thickness of the amorphous phase between lamellae (and hence a different length of the confined region). They reported an increase in the volume fraction of crystals and the thickness of the amorphous phase with increasing crystallization temperature (T_c). Dielectric loss measured at 1 Hz as a function of temperature decreased in intensity and increased in breadth with decreasing T_c , but the loss maximum remained at the same temperature. Unfortunately, their dielectric data were collected from temperature scans and not from frequency sweeps that are essential for a study of dynamics. This makes a direct comparison with our results difficult, though the un-

changed location of their dielectric loss maximum on the temperature scale can be considered loosely analogous to the constant τ observed in Figures 5 and 6. With regard to our results, the unchanged fragility together with the unchanged average relaxation time seems compelling to allow the following conclusion. We note an early work by Ngai and Roland, who showed that crystallinity exerts a negligible effect on fragility (or cooperativity), expressed in terms of the T_g -scaled temperature dependence of the segmental relaxation time, for several semicrystalline polymers.²⁶ That these segmental dynamics measures are not sensitive to the different degree of crystallinity implies that the relaxing segments are smaller than the thickness of the amorphous layers (i.e., the distance between lamellae). We may therefore conclude that the distance between lamellae is greater than the length of the primitive segment and the characteristic size of the cooperatively rearranging domain. This further implies that the length scale of the α process is less than 4 nm, a commonly observed thickness of the interlamellar amorphous phase within a long period in PLA²⁷ and other polymers.²⁸ This size of the relaxing segment is in agreement with the number of about 2–5 nm, recently reported in several investigations of the cooperative length scale in glass formers.²⁹ It would be undoubtedly interesting to complement our DRS data with the scattering and electron microscopic information about the size and fraction of crystalline and amorphous regions in our samples.

Conclusions

The following conclusions were made regarding the segmental α dynamics in poly(L-lactic acid) measured by DRS before, during, and after crystallization. The intensity and the dielectric relaxation strength of the α process decrease with increasing degree of crystallinity. The average relaxation time, however, remains unaffected by the formation of lamellar crystals. This was true for both melt and cold crystallization, notwithstanding the fact that the macroscopic morphology was different in these two cases. The temperature dependence of the average relaxation time for samples that range from wholly amorphous to crystallized is represented by a single VFT function. The observed insensitivity of those segmental dynamics measures to the difference in the degree of crystallinity implies that the characteristic size of the cooperatively rearranging domains is less than the thickness of the amorphous layer between lamellae. It was concluded that the length scale of the α process in this PLA is less than 4 nm.

Acknowledgment. This material is based on work supported by the National Science Foundation under Grant DMR-0101182.

References and Notes

- (1) McCrum, N. G.; Read, B. E.; Williams, G. *Anelastic and Dielectric Effects in Polymeric Solids*; Wiley: London, 1967.
- (2) Boyd, R. H. *Polymer* **1985**, *26*, 323.
- (3) Boyd, R. H. *Polymer* **1985**, *26*, 1123.
- (4) For relevant discussion of crystallinity and morphology of polymers see, for example: Mandelkern, L. In *Comprehensive Polymer Science*; Allen, G., Bevington, J. C., Eds.; Pergamon: Oxford, 1989; Vol. 2, p 363. Vaughn, A. S.; Bassett, D. C. *Ibid.* Vol. 2, p 415. Sadler, D. M. *Ibid.* Vol. 1, p 731. Keller, A.; Goldbeck-Wood, G. *Ibid.*, 2nd Suppl.; Agarwal, S., Russo, S., Eds.; Elsevier Sci. Publ.: Oxford, 1996; p 241.

- (5) Riande, E.; Saiz, E. *Dipole Moment and Birefringence of Polymers*; Prentice Hall: Englewood Cliffs, NJ, 1992.
- (6) This work was never properly published in a separate article and the reader is referred to: Williams, G. *Adv. Polym. Sci.* **1979**, *33*, 60.
- (7) Grebowicz, J.; Lau, S. F.; Wunderlich, B. *J. Polym. Sci., Polym. Symp.* **1984**, *71*, 19.
- (8) Suzuki, H.; Grebowicz, J.; Wunderlich, B. *Makromol. Chem.* **1985**, *186*, 1109.
- (9) Huo, P.; Cebe, P. *Macromolecules* **1992**, *25*, 902.
- (10) Huo, P.; Cebe, P. *J. Polym. Sci., Part B: Polym. Phys.* **1992**, *30*, 239.
- (11) Mijovic, J.; Sy, J. W.; Kwei, T. K. *Macromolecules* **1997**, *30*, 3042 and references therein.
- (12) Sy, J. W.; Mijovic, J. *Macromolecules* **2000**, *33*, 933 and references therein.
- (13) Ezquerro, T. A.; Roslaniec, Z.; Lopez-Cabarcos, E.; Balta-Calleja, F. J. *Macromolecules* **1995**, *28*, 4516.
- (14) (a) Fitz, B.; Andjelic, A.; Mijovic, J. *Macromolecules* **1997**, *30*, 5227. (b) Mijovic, J.; Miura, N.; Monetta, T.; Duan, Y. *Polym. News* **2001**, *26*, 251.
- (15) (a) Wunderlich, B. *Macromolecular Physics*; Academic Press: New York, 1976; Vols. 1–3. (b) Bassett, D. C. *Principles of Polymer Morphology*; Cambridge Press: Cambridge, UK, 1981.
- (16) The fundamental aspects of DRS, theoretical and experimental, will not be discussed here. For recent reviews the interested reader is referred to: (a) Williams, G. Dielectric relaxation spectroscopy of amorphous polymer systems: the modern approaches. In *Keynote Lectures in Selected Topics of Polymer Science*; Riande, E., Ed.; CSIC: Madrid, 1997; Chapter 1, pp 1–40. (b) Williams, G. Theory of Dielectric Properties. In *Dielectric Spectroscopy of Polymeric Materials*; Runt, J. P., Fitzgerald, J. J., Eds.; American Chemical Society: Washington, DC, 1997; Chapter 1, pp 3–65.
- (17) Stockmayer, W. H. *Pure Appl. Chem.* **1967**, *15*, 539.
- (18) Baysal, M. B.; Stockmayer, W. H. *Macromolecules* **1994**, *27*, 7429.
- (19) Massalska-Arodz, M.; Williams, G.; Thomas, D. K.; Jones, W. J.; Dabrowski, R. *J. Phys. Chem. B* **1999**, *103*, 4197.
- (20) Jackson, C. L.; McKenna, G. B. *J. Chem. Phys.* **1990**, *93*, 9002.
- (21) Stannarius, R.; Kremer, F.; Arndt, M. *Phys. Rev. Lett.* **1995**, *75*, 4698.
- (22) Arndt, M.; Stannarius, R.; Groothues, H.; Hempel, E.; Kremer, F. *Phys. Rev. Lett.* **1997**, *79*, 2077.
- (23) Kranbuehl, D. E.; Verdier, P. H. *J. Chem. Phys.* **1997**, *106*, 4788.
- (24) Adam, G.; Gibbs, J. H. *J. Chem. Phys.* **1965**, *43*, 139.
- (25) Schick, C.; Donth, E. *Phys. Scr.* **1991**, *43*, 423.
- (26) Ngai, K. L.; Roland, C. M. *Macromolecules* **1993**, *26*, 2688.
- (27) Tsuji, H.; Horii, F.; Nakagawa, M.; Ikada, Y.; Odani, H.; Kitamaru, R. *Macromolecules* **1992**, *25*, 4114.
- (28) Hsiao, B. S.; Sauer, B. B.; Verma, R. K.; Zachmann, G. H.; Seifert, S.; Chu, B.; Harney, P. *Macromolecules* **1995**, *28*, 6931.
- (29) Sillescu, H. *J. Non-Cryst. Solids* **1999**, *243*, 81.

MA0203647